# Flatness of Some DC Microgrid Topologies

Adam Kastner, Lutz Gröll, Veit Hagenmeyer
*Institute for Automation and Applied Informatics, Karlsruhe Institute of Technology*
Karlsruhe, Germany

***Abstract*—It is well-known that the state-space averaged models of buck and boost converters possess the property of differential flatness, which can prove beneficial to control design. This paper investigates the differential flatness of systems that consist of buck and boost converters interconnected at their outputs in three structures, which model DC microgrids with different properties. We present the mathematical form of potential flat outputs which depends on the number of converters of each type. Flatness-based feedforward control is demonstrated in simulations for all three types of interconnection. A numerical solution of the implicit flat parametrization is used where the explicit flat parametrization is not available.**

***Index Terms*—DC microgrid, differential flatness, feedforward control, boost converter, buck converter**

## I. Introduction

DC microgrids provide new options for the distribution of electrical power, especially in cases where power generation and consumption is already associated with DC devices, such as photovoltaic cells [1]. Whenever multiple power generators feed into the bus via DC converters, control algorithms are needed to provide load sharing between the sources while maintaining constant bus voltage. We propose that for grids that are differentially flat, flatness-based feedforward may be used to readjust the load sharing while minimizing the effect on the bus voltage during the transition.

Differential flatness is a concept originally introduced in [2], and is closely linked to feedback linearizability [3]. It allows the parametrization of the trajectories of all system variables, i.e. states, inputs, and outputs, based on an arbitrarily chosen trajectory for the so-called flat output. In control applications, flatness is especially useful in tracectory planning, where the invertibility problems of nonminimum phase systems are avoided, and optimal control problems can be reformulated. Further uses include trajectory tracking using tracking observers, and feedforward linearization.

The flatness properties of models of different types of switching power converters on their own have been analyzed by e.g. [4], [5], [6], and series interconnection of two boost converters is investigated in [7]. Flatness-based control approaches have been investigated for interleaved boost converters [8], [9] which are modeled equivalently to one of the grid models in this paper, but there time-scale separation has been used to consider the flatness of current and voltage dynamics separately. A similar time-scale separation approach is also used for a modular power flow controller for DC microgrids in [10]. Flatness-based optimal control has been investigated also for a particular DC microgrid system with three bidirectional buck-boost converters [11]. The differential flatness of buck converters connected to a common bus with capacitive storage was recently investigated in [12]. The buck converter model is linear, and the inclusion of boost converters with a bilinear model, as well as considering multiple grid topology models with an arbitrary number of nodes is the goal of the present paper.

In Section II, the three models of interconnection and the concept of differential flatness are described. Section III provides the system equations for the DC microgrids, and discusses the flatness and possible flat outputs. Examples of a flatness-based feedforward for a setpoint change are given for all three topologies in Sec. IV.

## II. Underlying Concepts

### A. Systems of Interconnected DC Converters

For the model of a grid of DC converters interconnected at their outputs, we consider the state-space averaged [13], or equivalently first-order averaged [14], models of buck and boost converter. Each converter is assumed to have an individual output capacitor, and the load is modeled as purely resistive.

We examine three different models for the interconnection of the DC converters, shown in Fig. 1.

**Output-paralleled** Direct parallel connection of converter outputs, which models a DC microgrid with negligible line resistances, or can also represent interleaved converters [8], [9].

**Resistive grid** Converters in connection with a purely resistive grid. Nonnegligible line impedances in the DC microgrid are included using the quasi-stationary line model [12].

**Capacitive storage** Converters in a grid that employs bus-connected capacitive storage. This case models a DC microgrid where in addition to loads, there is also capacitive storage attached directly to the bus to reduce voltage fluctuations [1].

### B. Differential Flatness

We give a definition for differential flatness based on the differential geometric view introduced in [15]. The definition is given for systems in an explicit form with a distinction between state and input variables, but a definition for implicit systems without this distinction is also possible [16].

**Definition 1** (Differential flatness [3])
A system $\dot{x} = f(x, u)$ defined on a smooth $n$-dimensional manifold $X$ with $u \in \mathbb{R}^m$ is called differentially flat at a point

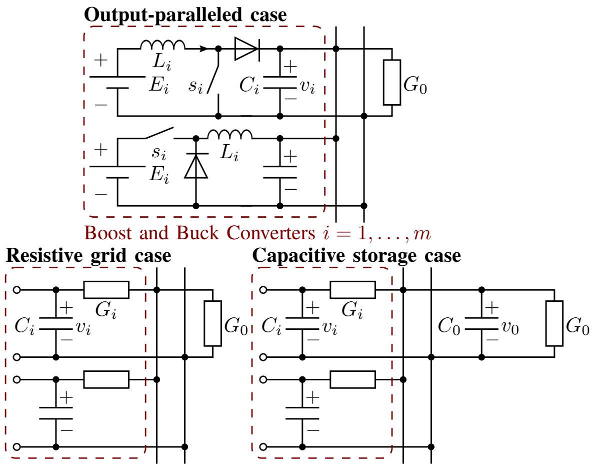


Fig. 1. Types of Interconnection

$(x_f, \bar{u}_f) \coloneqq (x, u, \dot{u}, \dots) \in X \times \mathbb{R}^m_\infty$ if is possible to define a virtual flat output

$$z = \psi(x, u, \dot{u}, \dots, u^{(q)}), \tag{1}$$

in a neighborhood of $(x_f, \bar{u}_f)$ depending on state, input and a finite number $q$ of input derivatives, such that the elements of $z$ are locally differentially independent in a neighborhood of $z_f = \psi(x_f, \bar{u}_f)$ and in this neighborhood there exists a parametrizing map

$$x = \varphi_x(z, \dot{z}, \dots, z^{(\ell-1)}), \quad u = \varphi_u(z, \dot{z}, \dots, z^{(\ell)}) \tag{2}$$

that depends only on $z$ and a finite number of $z$-derivatives, such that

$$\frac{\mathrm{d}\varphi_x(\bar{z})}{\mathrm{d}t} = f(\varphi_x(\bar{z}), \varphi_u(\bar{z})) \tag{3}$$

is identically satisfied.

The flat output is not necessarily the same as the system output, and also not unique. When choosing which flat output to use for a control application, it is advantageous if controlled variables are components of the flat output, and also if the number of derivatives $\ell$ needed for the parametrization is low.

As [16] points out, an explicit analytical form of the parametrization does not necessarily exist, and in general an implicit equation

$$\Phi(y, z, \dot{z}, \ddot{z}, \dots) = 0, \tag{4}$$

needs to be solved for $y = [x^\top, u^\top]^\top$. This is possible when $\frac{\partial \Phi}{\partial y}$ is nonsingular due to the implicit function theorem. We employ numerical solution of (4) to obtain the trajectories in $x, u$ when an explicit form cannot be obtained by the computer algebra tools of the *MATLAB Symbolic Math Toolbox* in our examples.

There exists no general test to determine whether a nonlinear system with multiple input variables is flat or not. Differential flatness is equivalent to dynamic feedback linearizability. A necessary and sufficient condition for static feedback linearizability of affine systems

$$\dot{x} = f(x) + \sum_{i=1}^{m} g_i(x) u_i, \quad x \in \mathbb{R}^n \tag{5}$$

with $f, g$ in $C^\infty$ was introduced by [17].

**Theorem 1** (Condition for static feedback linearizability [17], [18])
An affine system (5) is static feedback linearizable if and only if $\mathcal{Q}_i$ is involutive and of constant rank for $i = 0, \dots, n-1$, where

$$\mathcal{Q}_0 = \operatorname{span}\{g_1, \dots, g_n\}, \quad \mathcal{Q}_{i+1} = \overline{\mathcal{Q}_i} + \operatorname{ad}_f^{i+1} \mathcal{Q}_0 \tag{6}$$

and $\dim \mathcal{Q}_{n-1} = n$.

While static and dynamic feedback linearizability are equivalent for single-input systems [18], they are not for multiple-input systems. Thus, Thm. 1 only provides a sufficient condition for flatness in the multiple-input case. A necessary condition is provided by the ruled manifold criterion.

**Theorem 2** (Ruled manifold criterion [16])
If an implicit system

$$F(x, \dot{x}) = 0_m \tag{7}$$

is flat, then for all $(x, \dot{x})$ satisfying (7), there exists a vector $a$ such that

$$F(x, \dot{x} + \lambda a) = 0_m \quad \forall \lambda \in \mathbb{R}. \tag{8}$$

However, because the static feedback linearizability condition (6) is only sufficient, and the ruled manifold condition (8) is only necessary for differential flatness, neither can provide a definitive statement about flatness or nonflatness for arbitrary systems.

## III. Flatness of Interconnected DC Converters

For all three interconnection models, we consider systems that consist of a total of $m$ converters, with $q$ boost converters, and $m - q$ buck converters.

The system states $x_i$, $i = 1, \dots, n$ represent inductor currents and capacitor voltages, and the input signals $u_j$, $j = 1, \dots, m$ represent the pulse-width modulation (PWM) duty ratios in the individual converters. Note that for the boost converters, the input signal represents the proportion of each PWM cycle where the switching element is turned off, this is to simplify the equations by having $u$ appear instead of $(1 - u)$.

### A. Output-Paralleled Converters

For the case of output-paralleled converters, all capacitors act as one with the capacitance $C_0 = \sum_{i=1}^m C_i$, resulting in a system

$$L_i \dot{x}_i = E_i - x_n u_i, \qquad i = 1, \dots, q \tag{9a}$$

$$L_j \dot{x}_j = -x_n + E_j u_j, \qquad j = q+1, \dots, m \tag{9b}$$

$$C_0 \dot{x}_n = \sum_{j=q+1}^{m} x_j - G_0 x_n + \sum_{i=1}^{q} x_i u_i \tag{9c}$$

with $n = m + 1$ states, where the states $x_i$ and $x_j$ are the inductor currents of the boost converters and buck converters, respectively, and $x_n$ is the capacitor voltage.

Because the system is input-affine with one more state variable than inputs and linearly controllable, it is flat [18]. With at least one boost converter, i.e. $q > 0$,

$$z = \begin{bmatrix} L_1 x_1^2 + C_0 x_n^2 & x_2 & \dots & x_m \end{bmatrix}^\top . \tag{10}$$

can be used as a flat output. The first component is similar to the energy stored by a singular boost converter, which is well known to be a flat output for that case [4]. If there is at least one buck converter in the system, i.e. $q < m$, another possible flat output is

$$z = \begin{bmatrix} x_1 & x_2 & \dots & x_{m-1} & x_n \end{bmatrix}^\top . \tag{11}$$

Using the flat output (11) may be preferable over (10) for control design since the bus voltage $x_n$ is a component of the flat output.

### B. Resistive Grid

For the case of a purely resistive grid, the overall system model

$$L_i \dot{x}_i = E_i - x_{m+i} u_i, \qquad i = 1, \dots, q \tag{12a}$$

$$L_j \dot{x}_j = -x_{m+j} + E_j u_j, \qquad j = q+1, \dots, m \tag{12b}$$

$$C_i \dot{x}_{m+i} = -\sum_{k=1}^{m} G_{ik} x_{m+k} + x_i u_i \tag{12c}$$

$$C_j \dot{x}_{m+j} = -\sum_{k=1}^{m} G_{jk} x_{m+k} + x_j \tag{12d}$$

has $n = 2m$ states, with the first $m$ states representing the inductor currents and the other states the capacitor voltages. The conductances $G_{ij}$ between the converters are obtained via Kron reduction of the system's nodal admittance matrix [19]. To this end, we express the relationship between the converter output voltages $v_C = \begin{bmatrix} x_{m+1} & \cdots & x_{2m} \end{bmatrix}^\top$ and the load voltage $v_0$ with the load-induced capacitor currents $i_C$ in vector-matrix notation as

$$\begin{bmatrix} i_C \\ 0 \end{bmatrix} = \begin{bmatrix} \operatorname{diag}(g) & -g \\ -g^\top & \sum_{k=0}^{m} G_k \end{bmatrix} \begin{bmatrix} v_C \\ v_0 \end{bmatrix}, \tag{13}$$

where $g$ is the column vector of line conductances and $\operatorname{diag}(g)$ is a square matrix with the line conductances on the main diagonal. From the Kron reduction, we obtain

$$i_C = \big(\operatorname{diag}(g) + g(\sum_{k=0}^{m} G_k)^{-1} g^\top\big) v_C = G v_C \tag{14a}$$

$$v_0 = (\sum_{k=0}^{m} G_k)^{-1} g^\top v_C . \tag{14b}$$

More complex purely resistive networks can be simplified in a similar manner, with $v_0$ becoming a vector with an element for each load node.

This system is flat independent of the number of buck and boost converters and a flat output is given by

$$z = \begin{bmatrix} L_1 x_1^2 + C_1 x_{m+1}^2 \\ \vdots \\ L_q x_q^2 + C_q x_{m+q}^2 \\ x_{m+q+1} \\ \vdots \\ x_{2m} \end{bmatrix}, \tag{15}$$

where the components represent the energy stored in each boost converter and the output voltage of each buck converter. Because the parametrization of $x$ and $u$ requires solving a polynomial of a degree higher than 4 for $q > 1$, we numerically solve the implicit parametrization (4) for trajectory calculation in the example.

### C. Grid with Capacitive Storage

The model of the grid with capacitive storage

$$L_i \dot{x}_i = E_i - x_{m+i} u_i, \qquad i = 1, \dots, q \tag{16a}$$

$$L_j \dot{x}_j = -x_{m+j} + E_j u_j, \qquad j = q+1, \dots, m \tag{16b}$$

$$C_i \dot{x}_{m+i} = G_i (x_n - x_{m+i}) + x_i u_i \tag{16c}$$

$$C_j \dot{x}_{m+j} = G_j (x_n - x_{m+j}) + x_j \tag{16d}$$

$$C_0 \dot{x}_n = \sum_{k=1}^{m} G_k (x_{m+k} - x_n) - G_0 x_n \tag{16e}$$

has $n = 2m + 1$ states. The first $2m$ states are equivalent to those in the resistive grid case, and the state $x_n$ represents the voltage of the bus-connected capacitve storage. It is flat if there is at least one buck converter, and a flat output is given by

$$z = \begin{bmatrix} L_1 x_1^2 + C_1 x_{m+1}^2 \\ \vdots \\ L_q x_q^2 + C_q x_{m+q}^2 \\ x_{m+q+1} \\ \vdots \\ x_{2m-1} \\ x_n \end{bmatrix}. \tag{17}$$

Note that the flat output contains the bus voltage as a component, but not the output capacitor voltage of one of the buck converters.

The question of whether the system is flat or not with only boost converters ($q = m$) is still open, as there is no general test for flatness of mutliple-input nonlinear systems. Using the test introduced by [18], we can show that the system is not linearizable via static feedback. For $i, j = 1, \ldots, m$, we have

$$g_i = \begin{bmatrix} 0 \\ \vdots \\ 0 \\ -\frac{x_{m+i}}{L_i} \\ 0 \\ \vdots \\ 0 \\ \frac{x_i}{C_i} \\ 0 \\ \vdots \\ 0 \end{bmatrix}, \quad [g_i, g_j] = 0_n, \tag{18}$$

meaning that $\mathcal{Q}_0$ is involutive. However, for the distribution $\mathcal{Q}_1 = \overline{\mathcal{Q}_0} + \operatorname{ad}_f \mathcal{Q}_0$, we note that due to

$$\operatorname{ad}_f g_i = \begin{bmatrix} 0 \\ \vdots \\ 0 \\ \frac{G_i(x_{m+i}-x_n)}{C_i L_i} \\ 0 \\ \vdots \\ 0 \\ \frac{G_i x_i}{C_i^2} + \frac{E_i}{C_i L_i} \\ 0 \\ \vdots \\ 0 \\ -\frac{G_i x_i}{C_i C_0} \end{bmatrix}, \; [g_i, \operatorname{ad}_f g_i] = \begin{bmatrix} 0 \\ \vdots \\ 0 \\ \frac{2G_i x_i}{C_i^2 L_i} + \frac{E_i}{C_i L_i^2} \\ 0 \\ \vdots \\ 0 \\ \frac{G_i(x_n - 2x_{m+i})}{C_i^2 L_i} \\ 0 \\ \vdots \\ 0 \\ \frac{G_i x_{m+i}}{C_i C_0} \end{bmatrix}, \tag{19}$$

the distribution is not involutive, since $[g_i, \operatorname{ad}_f g_i] \in \overline{\mathcal{Q}_1}$ but $[g_i, \operatorname{ad}_f g_i] \notin \mathcal{Q}_1$. However, we cannot preclude flatness from this as it would be possible in the single-converter case. The ruled manifold criterion [16] can show nonflatness for some systems. For the system (16), eliminating the input $u$ from the system by solving (16a) for $u_i$ and inserting this into (16c) yields the implicit system

$$C_i \dot{x}_{m+i} = G_i(x_n - x_{m+i}) + \tfrac{x_i(E_i - L_i \dot{x}_i)}{x_{m+i}}, \quad i = 1, \ldots, m \tag{20a}$$

$$C_0 \dot{x}_n = \sum_{k=1}^{m} G_k(x_{m+k} - x_n) - G_0 x_n. \tag{20b}$$

Since these equations are linear in $\dot{x}$, there exists a vector $a \neq 0_n$ such that the equation holds true with $\dot{x} = \xi + \lambda a$ for all $\lambda \in \mathbb{R}$. Since there is no contradiction, the ruled manifold criterion also provides no statement about flatness or nonflatness of the system.

## IV. Examples of Flatness-Based Feedforward Control

In this section, we demonstrate in simulations how the property of differential flatness can be used to develop feedforward signals that transfer the interconnected system from one operating point $(x_\mathrm{a}, u_\mathrm{a})$ to another operating point $(x_\mathrm{b}, u_\mathrm{b})$ while keeping other variables, specifically the bus voltage, constant. Examples are given for all three cases, each time employing two boost converters and one buck converter. The parameters of the converters and transmission lines shared between cases are given in Tab. I. The line conductances are not used in the example for output-paralleled converters.

TABLE I
Example System Parameters

| | Value | | | Unit |
|---|---|---|---|---|
| $i$ | 1 | 2 | 3 | |
| $E_i$ | 100 | 150 | 400 | V |
| $L_i$ | 2 | 3 | 2 | mH |
| $C_i$ | 250 | 250 | 250 | µF |
| $G_i$ | 100 | 50 | 66.67 | S |
| $G_0$ | | | 0.33 | S |

TABLE II
Operating Points for the Output-Paralleled Example

| Operating Point a |
|---|
| $x_\mathrm{a} = [100.00, 66.70, 33.32, 300.00]^\top$ |
| $u_\mathrm{a} = [0.333, 0.500, 0.750]^\top$ |
| $z_\mathrm{a} = [100.00, 66.70, 300.00]^\top$ |
| **Operating Point b** |
| $x_\mathrm{b} = [150.00, 33.30, 33.35, 300.00]^\top$ |
| $u_\mathrm{b} = [0.333, 0.500, 0.750]^\top$ |
| $z_\mathrm{b} = [150.00, 33.30, 300.00]^\top$ |

### A. Example for Output-Paralleled Converters

In the example system for output-paralleled converters, the values of the three paralleled capacitances are summed to give $C_0 = 750\,\mu\mathrm{F}$. For the flatness-based trajectory design, we choose the flat output

$$z = \begin{bmatrix} x_1 & x_2 & x_4 \end{bmatrix}, \tag{21}$$

from which we can derive an explicit parametrization

$$x = \varphi_x(z, \dot{z}) \tag{22a}$$

$$u = \varphi_u(z, \dot{z}, \ddot{z}). \tag{22b}$$

The trajectory should transfer the system between the operating points given in Tab. II. For direct output-paralleled interconnection, the steady-state input depends only on the output voltage and not on the power sharing between the three converters. To obtain a continuous state trajectory, a third-order polynomial trajectory

$$z(t) = z_\mathrm{a} + (z_\mathrm{b} - z_\mathrm{a}) p(t/T), \quad \text{with } p(\tau) = -2\tau^3 + 3\tau^2, \tag{23}$$

is used for the flat output, with a transfer time of $2.5\,\mathrm{ms}$. Note that the second-order derivative is discontinous in at the start and end of the operating point transfer, and via (22b) this discontinuity can also appear in the input signal $u$. The state trajectories are shown in Fig. 2. Note how the voltage $x_4$ remains constant throughout the operating point transfer.

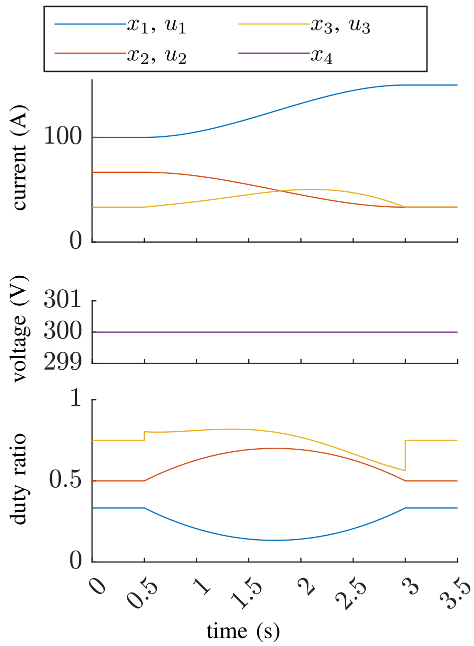


Fig. 2. Trajectories of the Output-Paralleled Example

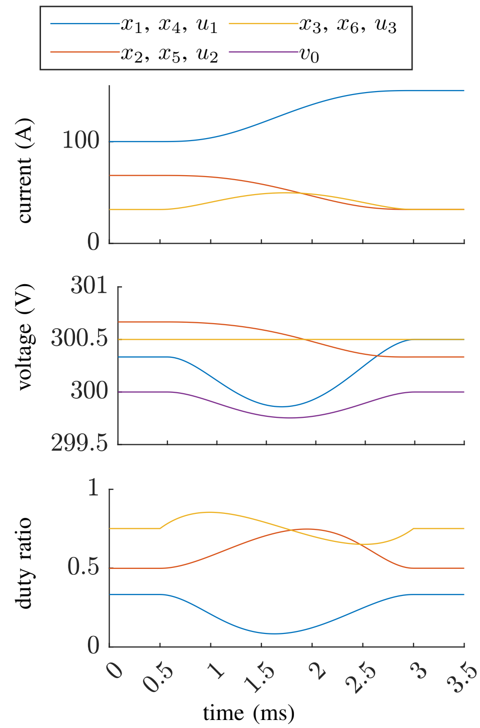


Fig. 3. Trajectories of the Resistive Grid Example

TABLE III
OPERATING POINTS FOR THE RESISTIVE GRID EXAMPLE

| |
|---|
| Operating Point a |
| $x_\mathrm{a} = [100.11, 66.81, 33.33, 300.33, 300.67, 300.50]^\top$ |
| $u_\mathrm{a} = [0.3330, 0.4989, 0.7512]^\top$ |
| $z_\mathrm{a} = [21.30, 18.00, 300.50]^\top$ |
| Operating Point b |
| $x_\mathrm{b} = [150.25, 33.37, 33.33, 300.50, 300.33, 300.50]^\top$ |
| $u_\mathrm{b} = [0.3328, 0.4994, 0.7512]^\top$ |
| $z_\mathrm{b} = [33.86, 12.95, 300.50]^\top$ |

TABLE IV
OPERATING POINTS FOR THE CAPACITIVE STORAGE EXAMPLE

| |
|---|
| Operating Point a |
| $x_\mathrm{a} = [100.11, 66.81, 33.33, 300.33, 300.67, 300.50, 300.00]^\top$ |
| $u_\mathrm{a} = [0.3330, 0.4989, 0.7512]^\top$ |
| $z_\mathrm{a} = [42594.50, 35992.77, 300.00]^\top$ |
| Operating Point b |
| $x_\mathrm{b} = [150.25, 33.37, 33.33, 300.50, 300.33, 300.50, 300.00]^\top$ |
| $u_\mathrm{b} = [0.3328, 0.4994, 0.7512]^\top$ |
| $z_\mathrm{b} = [67725.19, 25890.77, 300.00]^\top$ |

### B. Example for Resistive Grid

A flatness-based feedforward is calculated to transfer the system between the operating points given in Tab. III within $T = 2.5\,\mathrm{ms}$ starting at $t = 0.5\,\mathrm{ms}$. Since the parametrization of $x$ and $u$ depends on derivatives of $z$ up to the second order, we use the polynomial trajectory

$$z(t) = z_\mathrm{a} + (z_\mathrm{b} - z_\mathrm{a})p(t/T), \quad \text{with } p(\tau) = 6\tau^5 - 15\tau^4 + 10\tau^3, \tag{24}$$

where $z_3 = x_6$ remains constant throughout the transfer. The state and input trajectories are shown in Fig. 3. Also included is the trajectory of the DC bus voltage $v_0$, which dips slightly during the operating point transfer. However, it is clearly visible that the parametrized trajectories for the buck converter current $x_3$ and control signal $u_3$ perform a compensation such that the buck converter output voltage $x_6$ stays constant, fulfilling the objective.

### C. Example for Grid with Capacitive Storage

In the example for a grid with capacitive storage, the bus-connected capacitance is chosen as $C_0 = 250\,\mu\mathrm{F}$. A feedforward signal for a transition between the operating points given in Tab. IV is designed. The same type of fifth-order polynomial trajectory (24) is used as for the resistive grid case, but a longer transition time of $T = 5\,\mathrm{ms}$ is chosen. The state and input trajectories are shown in Fig. 4. It is clear that the bus voltage $x_7$, which is a component of the flat output, stays constant throughout the transition.

## V. CONCLUSIONS AND OUTLOOK

Models of different DC microgrid topologies including both buck converters with linear dynamics and boost converters with bilinear dynamics are differentially flat. The exception is the grid with capacitive storage employing only boost converters, where no statement about flatness or nonflatness has been achieved. The inclusion of buck-converters in the grid is advantageous to the flatness-based control, since it enables the use of a flat output that includes the bus voltage as a component for the output-paralleled case and the capacitive storage case. This differential flatness property can be used to

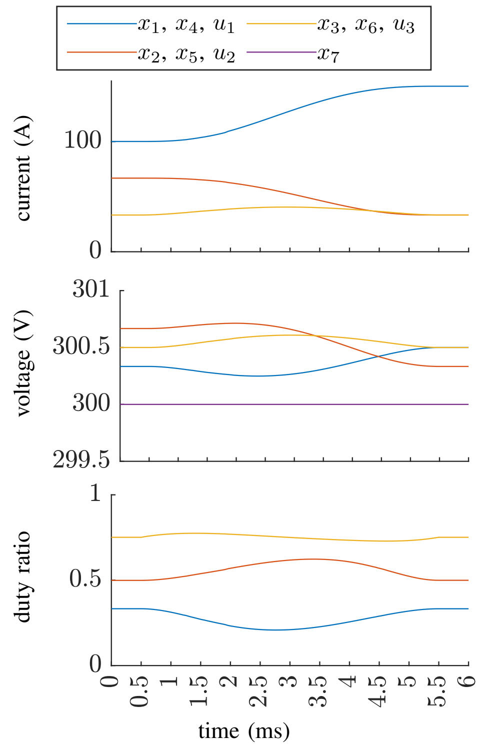


Fig. 4. Trajectories of the Capacitive Storage Example

design trajectories that perform a change in the distribution of power injection between the converters with minimal effect on bus voltage.

One drawback of the flatness-based feedforward control is that it requires centralized calculation, since the trajectories for the individual converters are interdependent. In addition, the local controllers of all converters require an absolute time reference to synchronize their coordinated control inputs. These drawbacks are shared with other types of feedforward control for wide-area systems.

In the present paper, we only consider the scenario where the variable to be maintained at a constant value is a component of the flat output. Other types of restrictions could be added and from the flat parametrization one would then obtain a differential or differential-algebraic equation in $z$ that can be solved as a boundary value problem.

## References


[1] A. T. Elsayed, A. A. Mohamed, and O. A. Mohammed, "DC microgrids and distribution systems: An overview," *Electric Power Systems Research*, vol. 119, pp. 407–417, 2015.

[2] M. Fliess, J. Lévine, P. Martin, and P. Rouchon, "Flatness and defect of non-linear systems: Introductory theory and examples," *International Journal of Control*, vol. 61, no. 6, pp. 1327–1361, 1995.

[3] J. Lévine, *Analysis and Control of Nonlinear Systems: A Flatness-Based Approach*. Berlin: Springer, 2009.

[4] A. Gensior, O. Woywode, J. Rudolph, and H. Güldner, "On differential flatness, trajectory planning, observers, and stabilization for DC-DC converters," *IEEE Transactions on Circuits and Systems I: Regular Papers*, vol. 53, no. 9, pp. 2000–2010, 2006.

[5] A. Gensior, J. Rudolph, and H. Güldner, "Flatness based control of three-phase boost rectifiers," in *European Conference on Power Electronics and Applications*. Dresden, Germany: IEEE, Sep. 2005, pp. 1–9.

[6] H. J. Sira-Ramírez and R. Silva-Ortigoza, *Control Design Techniques in Power Electronics Devices*. London: Springer, 2006.

[7] H. J. Sira-Ramírez and S. K. Agrawal, *Differentially Flat Systems*. New York: Marcel Dekker, 2004, no. 17.

[8] P. Thounthong and S. Pierfederici, "A new control law based on the differential flatness principle for multiphase interleaved DC–DC converter," *IEEE Transactions on Circuits and Systems II: Express Briefs*, vol. 57, no. 11, pp. 903–907, 2010.

[9] Y. Huangfu, Q. Li, L. Xu, R. Ma, and F. Gao, "Extended state observer based flatness control for fuel cell output series interleaved boost converter," *IEEE Transactions on Industry Applications*, vol. 55, no. 6, pp. 6427–6437, 2019.

[10] X. Lin-Shi, T. Simon, J.-F. Tregouet, and H. Morel, "Flatness-based control of an m-branch power flow controller for meshed DC microgrids," in *IEEE 1st International Power Electronics and Application Symposium (PEAS)*. Shanghai, China: IEEE, Nov. 2021, pp. 1–6.

[11] I. Zafeiratou, I. Prodan, L. Lefèvre, and L. Piétrac, "Meshed DC microgrid hierarchical control: A differential flatness approach," *Electric Power Systems Research*, vol. 180, p. 106133, 2020.

[12] F. Nicolau and A. Iovine, "Flatness of interconnected linear systems and applications to electrical systems," *IFAC-PapersOnLine*, vol. 55, no. 40, pp. 241–246, 2022.

[13] R. Middlebrook and S. Ćuk, "A general unified approach to modelling switching-converter power stages," *International Journal of Electronics*, vol. 42, no. 6, pp. 521–550, 1977.

[14] P. T. Krein, J. Bentsman, R. M. Bass, and B. L. Lesieutre, "On the use of averaging for the analysis of power electronic systems," *IEEE Transactions on Power Electronics*, vol. 5, no. 2, pp. 182–190, 1990.

[15] M. Fliess, J. Lévine, P. Martin, and P. Rouchon, "A Lie-Bäcklund approach to equivalence and flatness of nonlinear systems," *IEEE Transactions on Automatic Control*, vol. 44, no. 5, pp. 922–937, 1999.

[16] J. Rudolph, *Flatness-Based Control: An Introduction*. Düren: Shaker Verlag, 2021.

[17] B. Jakubczyk and W. Respondek, "On linearization of control systems," *Bulletin de l'Académie Polonaise des Sciences, Série des Sciences Mathématiques*, vol. 28, no. 9-10, pp. 517–528, 1980.

[18] B. Charlet, J. Lévine, and R. Marino, "On dynamic feedback linearization," *Systems & Control Letters*, vol. 13, no. 2, pp. 143–151, 1989.

[19] F. Dörfler, J. W. Simpson-Porco, and F. Bullo, "Electrical networks and algebraic graph theory: Models, properties, and applications," *Proceedings of the IEEE*, vol. 106, no. 5, pp. 977–1005, 2018.